Indian Journal of Radio & Space Physics
Vol. 24, August 1995, pp. 184-192

Electron densities in the equatorial lower ionosphere over Thumba and SHAR

H S S Sinha & Satya Prakash
Physical Research Laboratory, Navrangpura, Ahmedabad 380 009

Received 26 April 1995; accepted 23 May 1995

The paper presents the structures of the electron density profiles and the associated irregularities up to about 150 km over Thumba, India (8°52′ N, 76°87′ E, dip 0°47′ S) and up to about 340 km over SHAR, India (13°42′ N, 80°E, dip 14°N). These profiles were obtained using rocket-borne Langmuir probes and resonance probes. In all, profiles of 27 rocket flights conducted from Thumba and 6 from SHAR are presented. During the daytime normal electrojet (NEJ), the electron density profiles over Thumba were very smooth with only positive electron density gradients (i.e. the density increasing with increasing altitude). Increase in the density above 100 km altitude was much slower as compared to that below 100 km. During the daytime counter electrojet (CEJ), sharp layers of electron density, having a vertical extent of a few kilometres, were observed over Thumba. The nighttime profiles over Thumba show pronounced structures in the form of layers which are believed to be due to shears in the gravity wave winds. Morning and evening profiles over Thumba (around the twilight periods) show structures similar to the nighttime ones except that the peak densities are slightly smaller as compared to the nighttime values. The single daytime electron density profile available over SHAR during the NEJ period, shows the presence of a sharp layer around 90 km. The morning, evening and nighttime profiles over SHAR show a lot more structures as compared to the profiles over Thumba. These structures are believed to be due to the gravity waves.

1 Introduction

One of the most widely used rocket-borne probes for the measurement of electron density in the ionosphere is the Langmuir probe. A new version of Langmuir probe (LP) was developed at the Physical Research Laboratory (PRL), Ahmedabad, more than two decades back[1]. The PRL system has been extensively used and has yielded new results on the ionization irregularities in the D- and E-region of the equatorial ionosphere. The PRL's Langmuir probe (LP) has been flown on more than thirty rockets launched from Thumba and SHAR. It is well known that the retrieval of electron density from the current collected by the Langmuir probe is quite complex. This is so, because the conversion factor depends on many parameters such as the size of the probe, orientation of the probe with respect to magnetic field, sensor potential, electron temperatures, etc. Inadequate knowledge of these parameters leads to some uncertainty in the electron density values which are obtained using a single altitude-dependent calibration factor for a number of flights. Notwithstanding the limitations of the Langmuir probe for the measurement of the absolute electron densities, which are too well known, the probe gives an excellent idea of the gross features of the ionospheric electron density profiles during different times of the day. The calibration factor, used for the electron density profiles presented in this paper, was estimated using the ionosonde data as well as the mutual admittance probe which gives the absolute values of the electron density. The electron density profiles have been obtained for an equatorial station Thumba as well as for a low latitude station SHAR. These electron density profiles show a very consistent behaviour during different parts of the day and would, therefore, serve a very strong testing ground for ionospheric models such as International Reference Ionosphere (IRI).

2 Techniques

2.1 Rocket-borne Langmuir probe

In the rocket-borne Langmuir probe experiment, a metallic electrode, known as sensor, is exposed to the plasma. The LP sensor is usually kept at a few volts higher (positive) with respect to the plasma potential for the electron density measurements. The current collected by the probe

can then be approximated to the ambient electron density. The exact equations for the probe characteristics are known only for a few sensor shapes[2,3]. The probe theory is too complicated and excellent articles are available[4-6] which deal with, in detail, various aspects such as the size of the sensor, effects of collision of electrons with neutrals, rocket velocity, magnetic aspect, vehicle wake, contact potential, photoelectric effect, presence of negative ions in the ionosphere, etc. The LP system developed at PRL has few distinct advantages over the earlier versions, which are discussed in detail by Prakash and Subbaraya[1]. The most important advantage is that (a) the electrode is directly connected to the input of the current amplifier so that there is no leakage of current in the system as was happening earlier, (b) the reference of the current amplifier and the guard electrode is given the same voltage. In this system the leakage current is reduced by more than two orders of magnitude resulting in much higher frequency response of the system. It is this feature which has resulted in the use of PRL system for studying electron density irregularities as small as one metre scalesize in the vertical direction. Although the precise equations for the probe current are available for a few sensor shapes, it is not possible to quantitatively estimate many parameters coming into the equations. The probe current is, therefore, usually multiplied by a calibration factor which is determined by using some independent electron density measurement such as a propagation experiment, a mutual admittance probe, an ionosonde, etc. The PRL's LP system has been calibrated (i) by using the electron density derived from the critical frequency of the E-layer as observed with an ionosonde and (ii) by using the absolute electron density measurements using *in situ* mutual admittance probe. The calibration factor estimated for this system[7] for altitudes between 90 and 150 km agrees fairly well with other experiments[8]. The mutual admittance probe data which have been used in arriving at this calibration factor are described by Pandey[9]. Figure 1 shows the altitude dependent calibration factor (electron density/probe current) used by various workers for the electron density profiles from Thumba. In absence of any suitable calibration factor above 150 km altitude, a fixed factor (1 μA of probe current corresponds to 7.14×10^3 electron cm^{-3}) has been used by various workers for all altitudes for RH-560 flight results. In absence of any experimental values of absolute electron densities above 150 km over SHAR, use of a constant calibration factor seems to be a reasonable assumption. This is so, because above 150 km the collisions are drastically reduced and the ambipolar diffusion dominates. Any variation in probe current would depend on $T_e^{1/2}$. The variations in electron temperature (T_e) in 150-300 km are usually small.

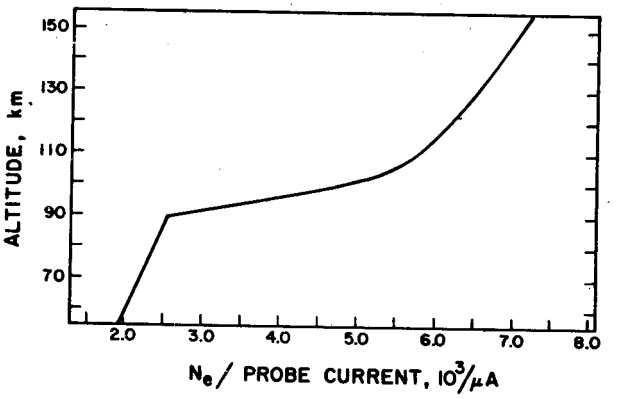

Fig. 1—Variation of the calibration factor with altitude [Calibration factor has a value 5 at 100 km altitude indicating that 1 microampere of current corresponds to 5×10^3 electrons cm^{-3} (Ref. 7)]

2.2 Rocket-borne mutual admittance probe

A mutual admittance probe system was developed at PRL to estimate absolute values of the electron density[10,11]. In this technique a RF signal of varying frequency in the range of 0.5-5.0 MHz is applied to an exciter antenna which is mounted on the rocket body in the form of a concentric ring. The induction field from the exciter is received near the nose tip of the rocket (see Fig. 2). As the frequency of the transmitted signal is varied, the received signal shows amplitude variations due to varying response of medium and several plasma resonances can be detected. The strongest resonance is observed at the upper hybrid frequency f_T which is given by

$$f_T^2 = f_N^2 + f_H^2$$

where, f_N is the plasma frequency and f_H the electron gyrofrequency of the medium. Once f_T is identified, the plasma frequency f_N can be calculated (by substituting the value of f_H which can be calculated) which directly yields the absolute value of the electron density in the medium. As shown in Fig. 3 plasma resonances obtained in this experiment[11] were very sharp enabling one to estimate plasma frequency very accurately. The data from two mutual admittance probe flights con-

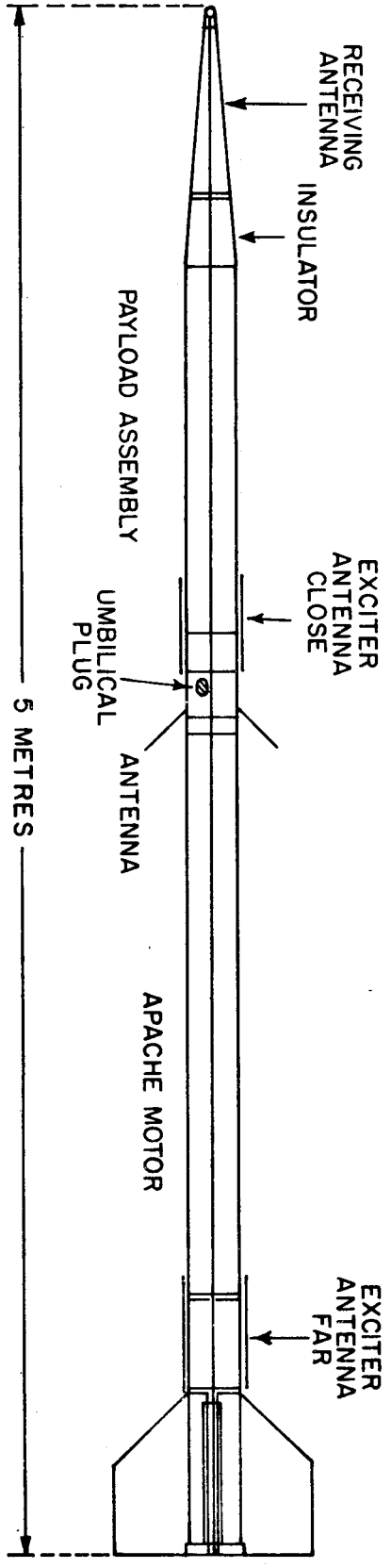

Fig. 2—Schematic of the mutual admittance probe on a sounding rocket (Ref. 11)

ducted from Thumba have been used to estimate the calibration factor for the LP. The electron density profiles obtained using the mutual admittance probe are presented along with the other profiles obtained by the Langmuir probe in the following section.

3. Electron density variation in the electrojet region

The electron density profiles obtained during the ascent of all rocket flights conducted from Thumba are presented in this section. Though the descent data are also good on most of the occasions they are not presented here as, in general, descent data are not considered very reliable, because the LP sensor may come in the wake of the rocket.

3.1 Daytime profiles during normal electrojet

Except the last two profiles in Fig. 4(b), Fig. 4 [(a) and (b)] shows the electron density profiles obtained over Thumba in the daytime during the periods of normal electrojet, i.e. when the electrojet current flows in the eastward direction. The general nature of the electron density profiles can be described by a rapid increase in electron density up to about 75 km, a relatively slower increase up to about 85 km followed by a very rapid increase up to about 100 km beyond which the electron density remains practically constant. The direction of electron density gradient is always positive, i.e. electron density increases with increasing altitude. During daytime normal electrojet conditions, the profile never shows regions of negative electron density gradient. The peak density during daytime is typically of the order of 2×10^5 cm^{-3}. Typical values of the electron density gradient scale length, L, which is defined as

$$\frac{1}{L} = \frac{1}{n_e} \frac{dn_e}{dh}$$

(where, n_e is the electron density and h the altitude) range between 2.0 and 0.5 km below 100 km altitude[12]. These strong positive gradients in electron density make the region below 100 km unstable under the influence of gradient drift instability as well as neutral turbulence mechanism. Ionization irregularities have been observed extensively below 100 km region[12-14]. The irregularities produced through gradient drift instability in the scalesize range of 30-300 m have characteristic saw-tooth type shapes.

3.2 Daytime profiles during counter electrojet

Figure 4(b) shows the electron density profiles on flights CO 5.16 and CO.22 which were conducted during the period of counter electrojet. Both these profiles show the presence of very sharp layers of ionization. During the flight CO 5.16 the layer was observed at around 95 km while during C.22 it was observed at around 91 km. The half widths of these layers were 2.5 and 1 km, respectively. The peak density of the layer on both the occasions, was higher by a factor of about two as compared to the background electron density of about 5×10^3 cm^{-3}.

Similar sharp layers of ionization have been observed in midlatitudes[15] and explained in terms of compression of metallic ions by wind shear mechanism[16,17]. In view of the fact that the magnetic field is horizontal over the geomagnetic equator, it was believed that wind shear mechanism would be inoperative over geomagnetic equator. But it was shown by Kato[18] that if the curvature of the geomagnetic field lines is taken into account the wind shear theory can be applicable at the geomagnetic equator also, though with a much reduced efficiency as compared to midlatitudes. Assuming a two-dimensional gravity wave wind (in the E-W and vertical directions) it was shown by Anandrao *et al.*[19] that the convergence values of Kato[18] were overestimated. Later on, Prakash and Pandey[20] considered a three-dimensional gravity wave wind, in which a finite wavelength along the geomagnetic field lines was shown to be extremely important for shorting the polarization electric field produced by the gravity wave wind. It was shown by Prakash and Pandey[20] that the convergence for a given gravity wave is maximum near the geomagnetic equator. Using the theoretical expressions of convergence given by Prakash and Pandey[20], it was shown by Pandey *et al.*[21] that the sharp layers of ionization observed during counter electrojet period are produced by the compression of metallic ions by the three-dimensional gravity wave winds.

Unlike normal electrojet period, the electron density profiles during counter-electrojet periods have regions of negative electron density gradient and in these regions electron density irregularities in 30-300 m scalesize range produced by gradient drift instability are observed. The reason is that during the counter electrojet period the Hall

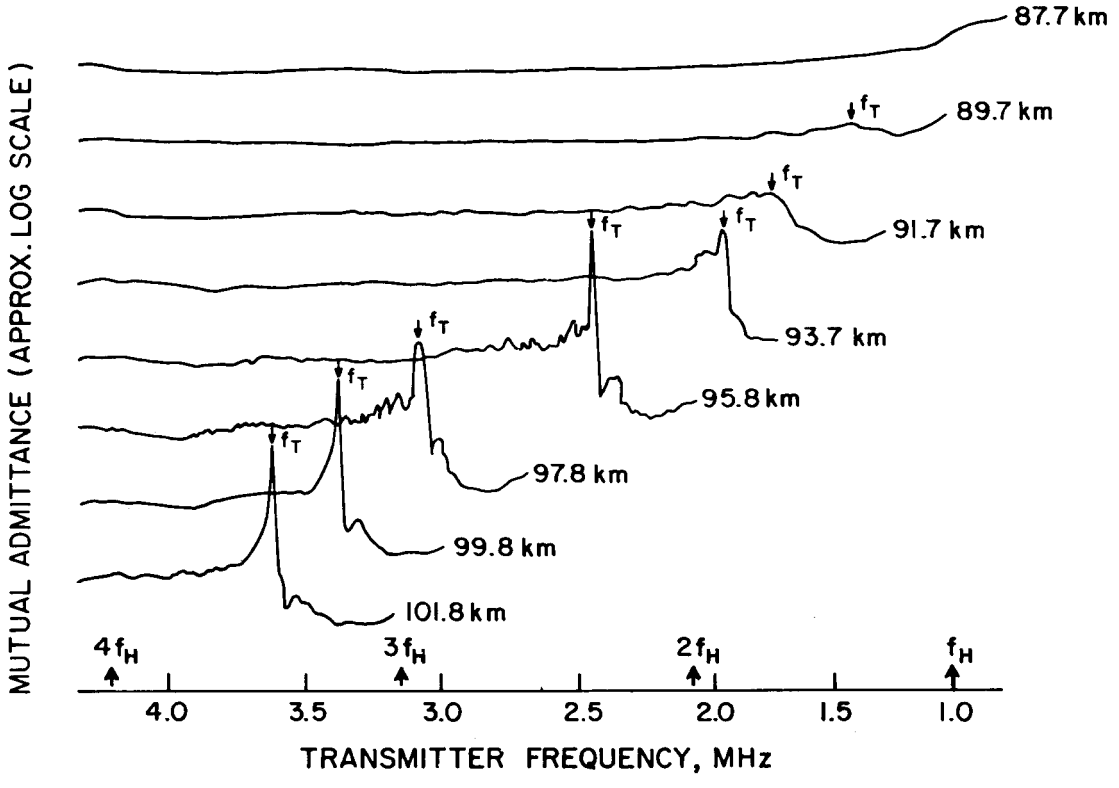

Fig. 3—A portion ot the mutual admittance probe data recorded between 87 and 102 km [The altitudes indicated inside correspond to the position of upper hybrid resonance (f_T) (Ref. 10)]

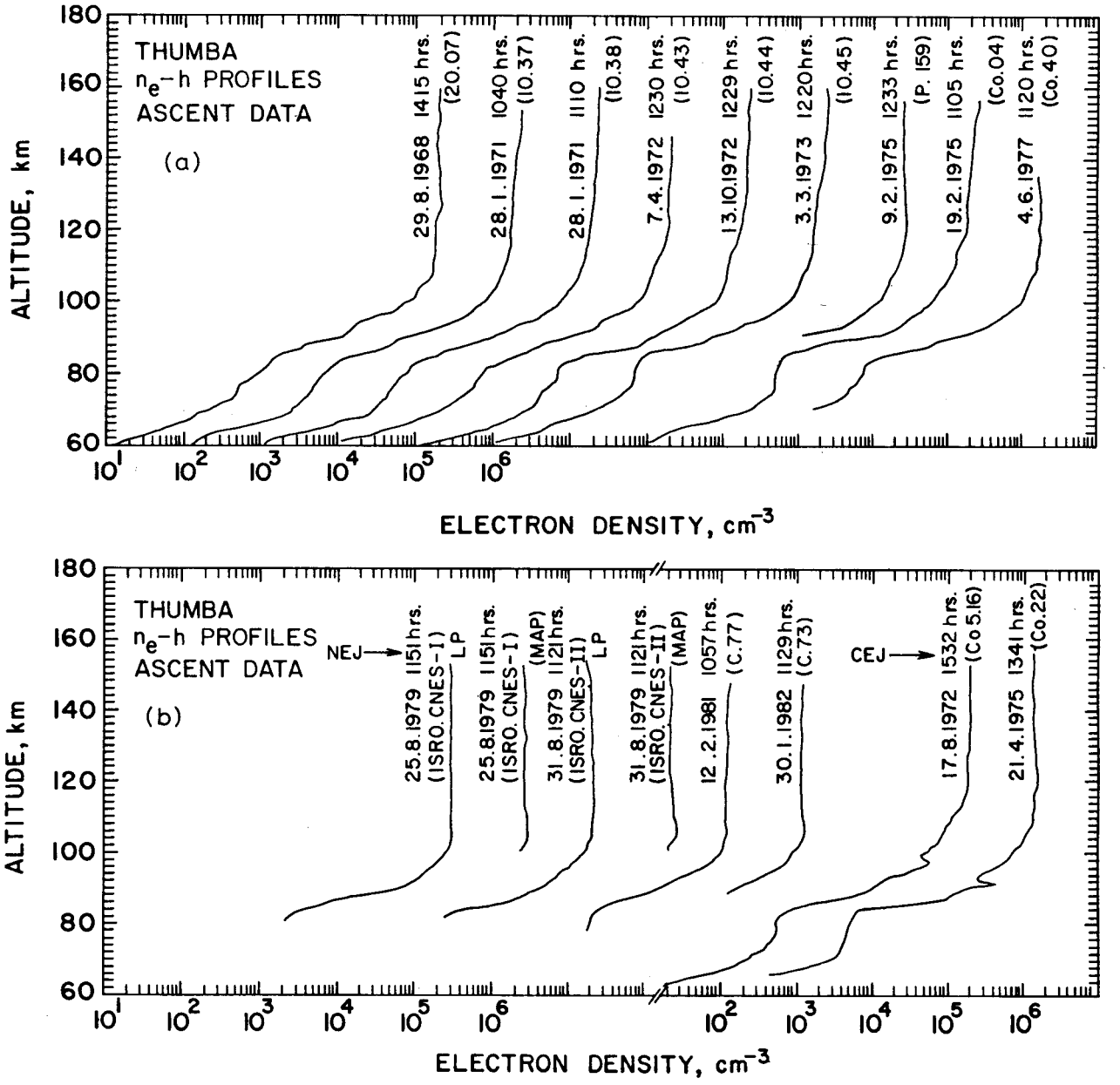

Fig. 4—(a) Electron density profiles of nine daytime flights conducted from Thumba during normal electrojet periods [Numbers within brackets indicate the flight number. Except for the first flight (No. 20.07) all the remaining profiles are shifted by one decade (on the X-axis) with respect to the previous flight for viewing convenience (Ref. 7, 11, 25, 30-33)]; and (b) Electron density profiles of nine daytime flights conducted from Thumba during normal electrojet periods and two daytime flights conducted during periods of counter electrojet. Other description is the same as Fig. 4(a) except that there is a separate scale for counter electrojet flights [Refs 9, 35, 36, 42)]

polarization field reverses its direction and becomes vertically downwards (during normal electrojet periods the Hall field is in vertically upward direction) allowing gradient drift instability to operate in the regions of negative density gradients[14].

3.3 Nighttime profiles

Figure 5 shows the electron density profiles obtained over Thumba during nighttime. All the flights were conducted within nearly two hours of the midnight. As the electron densities are lower during the nighttime, the probe current is also reduced during the night. Because of this, the Langmuir probe could measure densities only above 85 km during nighttime. Thus, there is practically very little ionization below 85 km. The electron

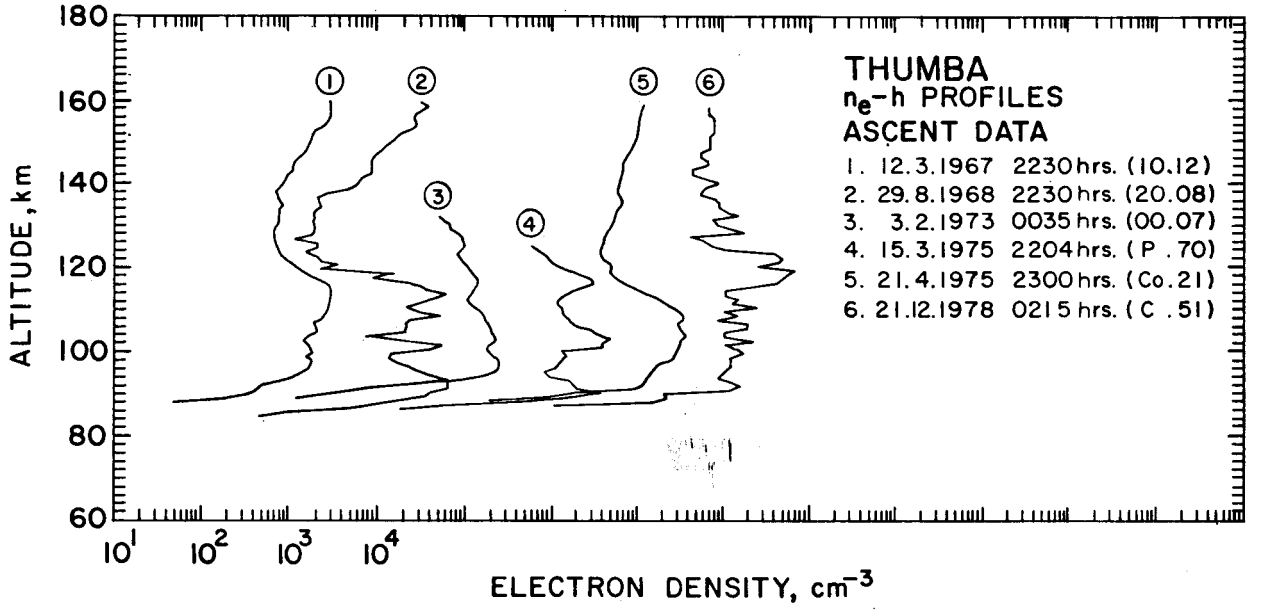

Fig. 5—Electron density profiles of six nighttime flights conducted from Thumba Other description same as Fig. 4(a) (Refs. 7, 22, 37)]

density increases rapidly in 85-95 km region reaching typically to about 10^3 cm^{-3} around 95 km. During the nighttime, the profiles show two very prominent features which are in contrast to daytime profiles. The first one is the presence of pronounced structures in the profile (see profile number 2 in Fig. 5) resulting a strong positive as well as negative electron density gradients. The gradient scalelength L ranges from $+0.5$ to -0.5. In fact, on many occasions, the profile gives an appearance of layers of ionization having thickness ranging from 0.5 km to a few kilometres. Density variations in these layers could be as large as one order of magnitude. This layered structure has high degree of variability in terms of the location of the layer as well as the density enhancements. These structures have been discussed extensively by many workers[18,20-24] and are now known to be due to the dynamic processes such as the gravity wave organization of the plasma. These structures indicate redistribution of the plasma and are not due to the photochemical process. Sharp layers of ionization wherein the electron density increases by a factor of 10 are seen very clearly during the ascent as well as the descent of the rocket, indicating that these layers have horizontal scalesizes in excess of 100 km.

During nighttime, electron density irregularities produced by gradient drift instability are observed in the negative density gradient regions, like the counter electrojet case.

3.4 Morning and evening periods profiles

Figure 6 shows the electron density profiles obtained over Thumba during morning and evening periods, respectively. Except the flight CO5.14 all other flights were conducted around the twilight periods, because these were simultaneously conducted with barium and sodium vapour release experiments which can be conducted around twilight only. Like the nighttime flights, the twilight flights also recorded electron densities only above about 80 km. During the twilight flights the electron density increases rapidly in the 85-95 km region and attains a typical value of about 5×10^3 cm^{-3} in 100-120 km region. These values are higher than the nighttime values in the same regions indicating that the solar radiation, which falls at grazing incidence, has produced ionization at these altitudes.

The electron density gradients are, in general, weak during twilight periods ($L \sim 5$ km) except in few small altitude ranges (of a kilometre or so), where L could be in the range of $+0.5$ km to -2 km. Electron density irregularities produced by gradient drift instabilities are occasionally observed in these strong density regions, if the direction of the gradient is parallel to the Hall polarization field.

Electron density profile of flight CO 5.14 which was conducted at 0745 hrs LT has all features very similar to a daytime profile[25,26].

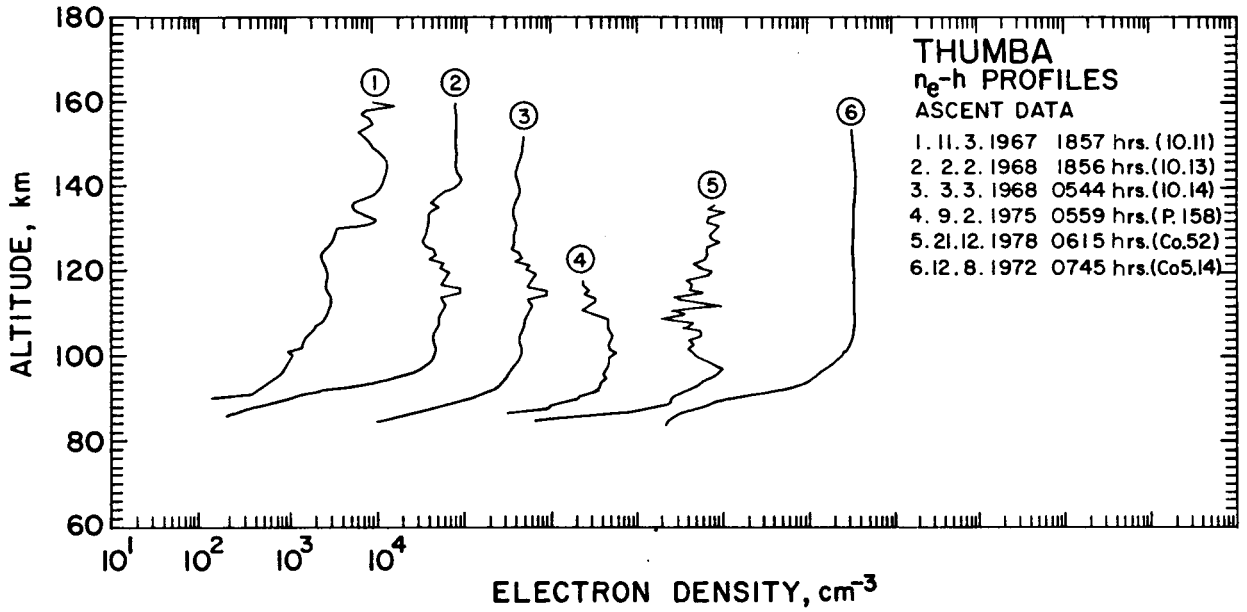

Fig. 6—Electron density profiles of two evening twilights flights, three morning twilight flights and one morning flight from Thumba. [Other description same as Fig. 4(a) (Refs. 7, 26, 38-40)]

4 Electron density variation outside the electrojet region

4.1 Daytime profiles

There has been only one daytime flight from SHAR which lies just outside the electrojet region. Figure 7 shows the electron density profile over SHAR obtained at 1010 hrs LT on 4 May 1987 (last profile). Presence of a small D-region is seen in the profile between 70 and 82 km. Above 82 km, the density increases monotonically up to about 100 km with only positive density gradients. At 100 km the presence of a very sharp layer of ionization, where the density increases by more than a factor 2 in a small vertical extent of about 2.0 km, can be seen very clearly. Beyond 100 km the profiles show very little variation in density up to the apogee which was around 300 km. Like the equatorial station Thumba, the gradient-drift-instability driven irregularities are also seen at SHAR in the region 90-100 km which is characterized by positive electron density gradients[27].

The presence of a sharp layer of ionization at 100 km over SHAR is a feature which is different from what is observed at Thumba at the same time. More daytime flights are required to throw more light on the existence and the mechanism of generation of these layers.

4.2 Nighttime profiles

There have been only three rocket launches from SHAR during the nighttime and all of these were conducted under the conditions of strong spread-F (Refs. 27, 28). Figure 7 shows the profile of the nighttime flights. All the three profiles show structures in the electron density in 100-140 km region. The vertical wavelength of some of these structures can be as large as 25 km over which the electron density varies by a factor ranging between 7 and 10. Many of these structures were similar during ascent and descent which are separated by 400 km (the descent profile are given elsewhere[27,28]) indicating that these could be due to gravity waves with east-west wavelengths comparable to the horizontal wavelengths of these structures.

Another feature in the nighttime profiles over SHAR, is the presence of a valley region around 130 to 150 km. The value of electron density remains low up to the base of F-region. The valley region is seen during ascent as well as descent[27,28]. This region is characterized by relatively low electron density of about 3×10^4 cm^{-3} and the absence of any significant structures. Only during the flight RH 560-25 a large-scale structure with vertical wavelength of about 100 km was observed in the valley region. The mechanism of generation of this large scale structure is not known. Probable causes could be (i) due to wind induced instability suggested by Chiu and Strauss[29]; but the observed electron density gradients appear to be much smaller than the required

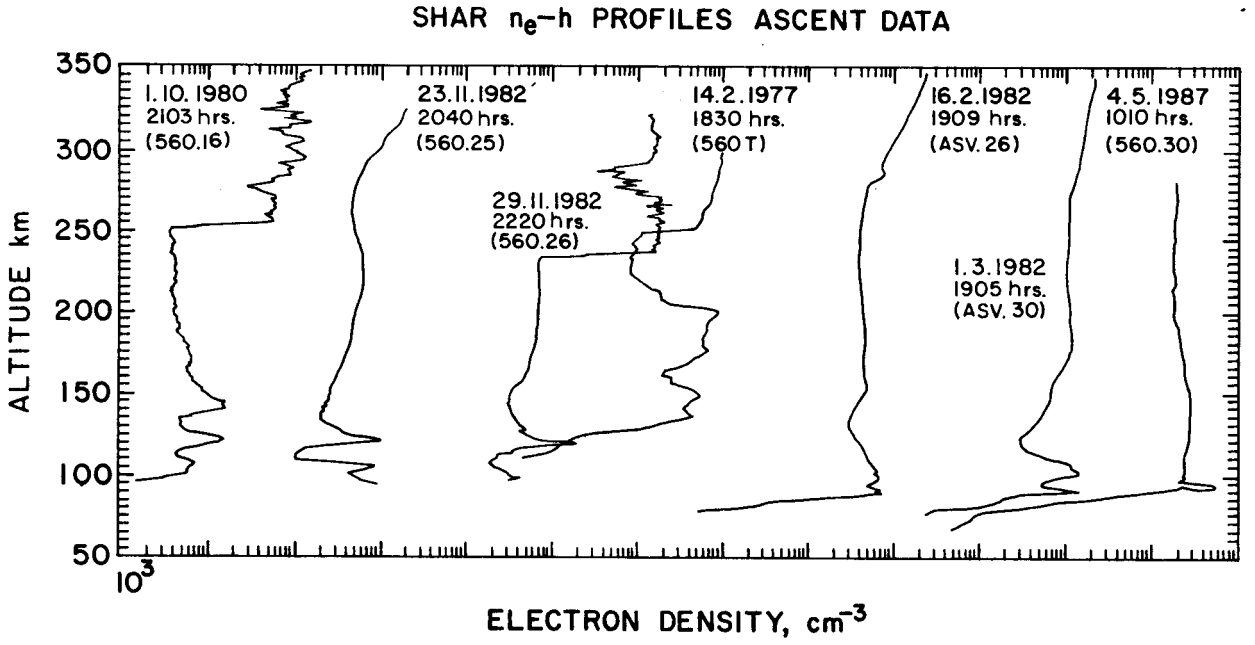

Fig. 7—Electron density profiles of three nighttime, three evening time and one daytime flight conducted from SHAR. [Except for the first flight (560.16) all the remaining profiles are shifted by two decades (on the X-axis) with respect to the previous flight for viewing convenience (Refs 7, 27, 28, 41)]

gradients by the theory, and (ii) it could be due to the transport of plasma by a gravity wave wind as suggested by Prakash and Pandey[20].

The nature of the base of the F-region was highly variable on all the three profiles. During the flight RH 560-16 the base was equally sharp during ascent and descent (for descent profile see Ref. 27). During the ascent the base was located at 250 km where the density increased by a factor of 10 in just 2.7 km, resulting in L values of 1.2 km. During the descent the base was located at 257 km and the density increased by a factor of 15 in 3 km yielding an L value of 0.9 km. In case of the flight RH 560-25 the base of the F-region was much higher than the apogee of the rocket, which, as shown by the SHAR ionogram, had a virtual height of 350 km. For the flight RH 560-26 the nature of the base of F-region was quite different during ascent and descent[28]. During the ascent the base was at 230 km where the electron density increased very steeply by as large as a factor of 18 in 0.8 km ($L \approx 0.8$ km). While during the descent the base could not really be sharply defined as electron density in 230 km region increases very slowly by a factor of 12 in 16 km ($L \sim 24$ km). Electron density irregularities with scalesizes range from a metre to a few tens of kilometres were observed both in the E-region and the F-regions in the negative electron density gradient region. Above the F-region base, one can see the presence of plasma depletions of various vertical widths and degree of depletion. On the flight RH 560-16 the plasma depletions were present during ascent as well as descent. The most prominent depletions were observed around 275 km wherein the electron density got depleted by a factor of 4 in a vertical distance (width) of about 15 km. Above 300 km, a large number of medium and small depletions were observed. For the E-region irregularities the gradient drift instability is the causative mechanism, whereas for the F-region irregularities both collisional Rayleigh Taylor and gradient drift instability contribute depending upon the altitude.

4.3 Evening time profiles

There have been only three evening time flights from SHAR which are also shown in Fig. 7. Unlike the evening time profiles over Thumba, the profiles over SHAR very clearly show the presence of sporadic-E layers in 90-110 km region. Electron density irregularities in the scalesize range 1 m to a few kilometres produced by the gradient drift instability were also seen in the positive density gradient regions. The valley in the electron density in 110-150 km region is also seen clearly. The peak electron density during the evening time is nearly 2×10^4 cm^{-3} which is more

than one order of magnitude smaller as compared to daytime density over SHAR.

5 Conclusion

A large number of rocket flights were conducted from Thumba which lies in the equatorial electrojet region and from SHAR which is just outside the influence of the equatorial electrojet. Electron density profiles during day, night, evening and morning times were presented for normal as well as counter electrojet periods. Gross features of the profiles specially from Thumba are fairly stable. The profiles of flights 10.37 and 10.38 which were conducted within an interval of 30 min show that the electron densities from the two flights agree within 10% at all altitudes. Considering the uncertainties in the calibration factor, for various reasons, the agreement between these two profiles is considered extremely good. This shows the repeatability of PRL's Langmuir probe performance. It is believed that the profiles presented in this paper will provide a substantial input to test the applicability of ionospheric models over equatorial and low latitude regions such as International Reference Ionosphere (IRI) model.

Acknowledgements

The authors would like to thank Prof. B H Subbaraya for his going through the entire manuscript and suggesting many improvements. Thanks are also due to Mr N Dutt, Mr S R Das and Dr K P Subramanian of PRL for their help in retrieving the density profiles from the published literature and putting them in a uniform format. This work was supported by the Physical Research Laboratory, Ahmedabad.

References

1 Prakash S & Subbaraya B H, *Rev Sci Inst (USA)*, 38 (1967) 1132.
2 Smith L G, *Technique manual on electron density and temperature measurements in the ionosphere*, edited by K Maeda (Kyoto University, Japan), 1964.
3 Brace L H & Spencer N W, *J Geophys Res (USA)*, 69 (1964) 4686.
4 Smith L G, *Small rocket instrumentation techniques*, edited by K I Maeda (North Holland Publishing Co Ltd, Amsterdam), 1969.
5 Langmuir I & Mott Smith H M, *G E C Rev (UK)*, 27 (1924) 449.
6 Mott Smith H M & Langmuir I, *Phys Rev (USA)*, 28 (1926) 727.
7 Subbaraya B H, Satya Prakash & Gupta S P, *Sci Rep No.*, ISRO, PRL-SR-15-83, Indian Space Research Organisation, 1983.
8 Mechtly E A, Bowhill S A, Smith L G & Knaebel H W, *J Geophys Res (USA)*, 72 (1967) 5239.
9 Pandey R, *Studies in Equatorial Aeronomy*, Ph D Thesis, Gujarat University, Ahmedabad, India, 1981.
10 Rao T R & Satya Prakash, *Space Res (USA)*, XVIII (1978) 281.
11 Satya Prakash, Subbaraya B H & Gupta S P, *Indian J Radio & Space Phys*, 1 (1972) 72.
12 Sinha H S S & Satya Prakash, *Indian J Radio & Space Phys*, 16 (1987) 102.
13 Sinha H S S, *J Atmos & Terr Phys (UK)*, 54 (1992) 49.
14 Sinha H S S, *Studies in Equatorial Aeronomy*, Ph D Thesis, Gujarat University, Ahmedabad, India, 1976.
15 Miller K L & Smith L G, *J Atmos & Terr Phys (UK)*, 39 (1977) 899.
16 Whitehead J D, *J Atmos & Terr Phys (UK)*, 20 (1961) 49.
17 Axford W I & Cunnold D H, *Radio Sci (USA)*, 1 (1966) 191.
18 Kato S, *J Geophys Res (USA)*, 78 (1973) 757.
19 Anandrao B G, Raghavarao R & Reddy C A, *J Geophys Res (USA)*, 82 (1977) 1510.
20 Prakash S & Pandey R, *Proc Indian Acad Sci*, 88A (1979) 229.
21 Pandey R, Prakash S & Sinha H S S, *J Atmos & Terr Phys (UK)*, 54 (1992) 63.
22 Subbaraya B H, Prakash S & Gupta S P, *Indian J Radio & Space Phys*, 9 (1981) 626.
23 Fejer B G, Farley D T, Balsley B B & Woodman R F, *J Geophys Res (USA)*, 80 (1975) 1313.
24 Fejer B G & Kelley M C, *Space Phys (USA)*, 18 (1980) 401.
25 Gupta S P & Satya Prakash, *Planet & Space Sci (USA)*, 27 (1979) 145.
26 Gupta S P, *Adv Space Res (UK)*, 12 (1992) 141.
27 Satya Prakash, Pal S, Pandey R & Subbaraya B H, *Adv Space Res (UK)*, 3 (1983) 195.
28 Satya Prakash & Pal S, *Adv Space Res (UK)*, 5 (1985) 39.
29 Chiu Y T & Strauss J M, *J Geophys Res (USA)*, 84 (1979) 3283.
30 Satya Prakash, Subbaraya B H & Gupta S P, *J Atmos & Terr Phys (UK)*, 33 (1971) 129.
31 Satya Prakash, Gupta S P, Subbaraya B H & Jain C L, *Nature (Phys. Sci) (UK)*, 233 (1971) 56.
32 Satya Prakash, Subbaraya B H & Gupta S P, *Methods of measurements and results of lower ionospheric structure*, edited by K Rawer (Academie-Verlag, Berlin) 1974, pp. 259-265.
33 Satya Prakash, Gupta S P, Subbaraya B H & Pandey R, *Adv Space Explor (USA)*, 8 (1980) 3.
34 Satya Prakash, Pal S & Pandey R, *Adv Space Res (UK)*, 3 (1983) 93.
35 Satya Prakash, Gupta S P, Sinha H S S & Rao T R, *Space Res (USA)*, XVI (1976) 401.
36 Satya Prakash, Gupta S P, Subbaraya B H & Pandey R, *Space Res (USA)*, XIV (1979) 279.
37 Satya Prakash, Gupta S P & Subbaraya B H, *Planet & Space Res (USA)*, 18 (1970) 1307.
38 Subbaraya B H, *Studies in Equatorial Aeronomy*, Ph D Thesis, Gujarat University, Ahmedabad, India, 1968.
39 Satya Prakash, Subbaraya B H & Gupta S P, *J Atmos & Terr Phys (UK)*, 30 (1968) 1193.
40 Satya Prakash, Subbaraya B H & Gupta S P, *Space Res (USA)*, IX (1969) 237.
41 Gupta S P, *Planet & Space Sci (UK)*, 34 (1986) 1081.
42 Satya Prakash & Pal S, *J Atmos & Terr Phys (UK)*, 47 (1985) 853.